CHAPTER 6

STUDY OF WAVE PROPAGATION IN AN INFINITE SOLID DUE TO LINE HEAT SOURCE UNDER MOORE-GIBSON-THOMPSON THERMOELASTICITY

6.1 Introduction[1]

The present Chapter is devoted to the study of a new thermoelasticity theory which is recently developed by Quintanilla (2019; 2020) as the combination (or generalization) of the Lord-Shulman and Green-Naghdi thermoelasticity theory of type III. This theory is based on the Moore-Gibson-Thompson (MGT) heat model in its linearized form and hence we refer this new thermoelastic model as Quintanilla-Moore-Gibson-Thompson (QMGT) model. LS and GN-III models are recovered when we omit the dependence with respect to suitable variables in QMGT model. MGT model is used for modeling of high amplitude sound wave. Kaltenbacher et al. (2011) has studied the fully non-linear version of MGT equation and gave the well-posedness and the exponential decay rates arising in high intensity ultrasound. The spectral analysis for this model is also carried out by Marchand et al. (2012). Lasiecka and Wang (2015; 2016), Dell'Oro et al. (2016) investigated how the memory term can influence the damping mechanism and causes

[1]The content of this chapter is published in *Acta Mechanica,* 232 (2021): 4747-4760.

energy decay on MGT system. Dell'Oro and Pata (2017) disscussed the exponential stability condition for MGT equation and its relation with linear viscoelasticity. In recent years, The QMGT model for thermoelasticity has gained great interest. The results on this model as discussed by Abouelregal et al. (2020), Bazzara et al. (2021a) and Abouelregal and Sedighi (2021) are worth mentioning here. The uniqueness of results and instability of some thermomechanical problems involving the Moore-Gibson-Thompson equation has been reported by Pellicer and Quintanilla (2020), while the interesting results on the decay of the energy for radial solutions in MGT thermoelasticity are provided by Bazzara et al. (2021b). Kumar and Mukhopadhyay (2020) applied the QMGT theory to understand the dynamic behaviour of a simply supported microbeam resonator.

The main motive of the present chapter is to investigate the dynamics of the solutions for the QMGT theory for isotropic elastic medium due to the presence of line heat source. It is worth to be mentioned here that eminent researchers like Sherief and Anwar (1986), Dhaliwal et al. (1997), Chandrasekhariah and Srinath (1998), Ezzat (1995) and Chandrasekharaiah et al. (1991), Prasad et al. (2011) investigated the thermoelastic interactions due to continuous line heat source on a linear, homogenous unbounded solid in the context of LS, GN-III, GN-II, GL, three phase-lags models, respectively. The effects of such heat source has been discussed in details for the MGL thermoelasticity in Subchapter 3.1. Some important observations about the responses of line heat source under MGL model have been pointed out there and the present Chapter is motivated to extend this concept and understand the effects of QMGT theory in presence of line heat source. We investigate the short-time approximated expressions for displacement, temperature and stress fields in physical time-space domain in the present context. We specially enumerate the points of discontinuity, velocity of thermal and elastic disturbances and analyse the dependency of field variables on various physical parameters under QMGT theory. The finite speed predictions for elastic as well

as thermal disturbance by the present thermoelastic model is identified analytically. Furthermore, the damping nature of elastic and thermal waves are shown analytically. The results of the present study are compared with the corresponding results of other thermoelastic models as mentioned above. The analytical results are verified with the numerical results of the present problem for a suitable example and it has been shown with graphical results that the field variables have no effect after the thermal wavefront, which verifies the correctness of our analytical results and reveals that QMGT model show finite domain of influence of the disturbance at any particular time. Similarity and dissimilarity in prediction of this model with other existing models are highlighted in detail.

6.2 Governing Equations

In this section, the formulation of the newly proposed thermoelasticity theory (QMGT) is presented by considering the basic equations in the presence of heat source for isotropic elastic medium in rectangular coordinate system.

The heat conduction equation as suggested by Quintanilla (2019) is given by

$$q + \tau_q \frac{\partial q}{\partial t} = -k\nabla T - k^*\nabla v \tag{6.2.1}$$

where

$$\dot{v} = T. \tag{6.2.2}$$

Here k and k^* are the thermal conductivity and conductivity rate respectively. In the above equation v represents thermal displacement, a new variable that is characteristic of GN-III and QMGT theories. A superposed dot denotes the partial differentiation with respect to time. In above equation, if we consider the case when τ_q vanishes, we recover GN-III model

We consider the equation of motion in absence of any body force as given by

$$\sigma_{ij,j} = \rho \ddot{u}_i \tag{6.2.3}$$

where the stress-strain-temperature relation is given by

$$\sigma_{ij} = \lambda e_{kk}\delta_{ij} + 2\mu e_{ij} - \gamma T \delta_{ij} \tag{6.2.4}$$

The energy equation in presence of heat source is taken as

$$-\nabla q = \rho c_v \frac{\partial T}{\partial t} + \gamma T_0 \frac{\partial e}{\partial t} - \rho Q \tag{6.2.5}$$

Combining Eqs. (6.2.1) and (6.2.5), we obtain the new heat conduction equation based on QMGT model in presence of heat source as

$$k\nabla^2 T + k^* \nabla^2 v = \left(1 + \tau_q \frac{\partial}{\partial t}\right)\left(\rho c_v \frac{\partial T}{\partial t} + \gamma T_0 \frac{\partial e}{\partial t} - \rho Q\right) \tag{6.2.6}$$

Taking time derivative in Eq. (6.2.6), we have

$$k\nabla^2 \dot{T} + k^* \nabla^2 T = \left(1 + \tau_q \frac{\partial}{\partial t}\right)\left(\rho c_v \frac{\partial^2 T}{\partial t^2} + \gamma T_0 \frac{\partial^2 e}{\partial t^2} - \rho \dot{Q}\right) \tag{6.2.7}$$

Further, by combining Eqs. (6.2.3) and (6.2.4), we have

$$\rho \ddot{u}_i = \left(2\mu e_{ij} + \lambda e_{kk}\delta_{ij}\right)_{,j} - \gamma T_{,j}\delta_{ij} \tag{6.2.8}$$

6.3 Problem Formulation

We consider the problem of an infinite thermoelastic medium. The medium is assumed to be homogenous and isotropic. Let us assume the body has an axisymmetric structure

under the axisymmetric load, so the problem is one-dimensional and the physical field variable displacement vector has only the radial component $u(r,t)$. The stress tensor has only two non-zero components σ_{rr}, $\sigma_{\phi\phi}$ that are in radial and transverse directions, respectively. Therefore, kinematic relations in cylindrical coordinate system (r,φ,z) are given by

$$e_{rr}=\frac{\partial u}{\partial r}, e_{\phi\phi}=\frac{u}{r}, e=\frac{\partial u}{\partial r}+\frac{u}{r}, \tag{6.3.1}$$

The equation of motion is therefore transformed to

$$\rho\frac{\partial^2 u}{\partial t^2}=\frac{\partial \sigma_{rr}}{\partial r}+\frac{\sigma_{rr}-\sigma_{\varphi\varphi}}{r}. \tag{6.3.2}$$

Using Eq. (6.3.1) in Eq. (6.2.4), one can obtain the components of stress tensors in the following forms:

$$\sigma_{rr}=(\lambda+2\mu)\frac{\partial u}{\partial r}+\lambda\frac{u}{r}-\gamma T \tag{6.3.3}$$

$$\sigma_{\phi\phi}=(\lambda+2\mu)\frac{u}{r}+\lambda\frac{\partial u}{\partial r}-\gamma T \tag{6.3.4}$$

Eqs. (6.2.7 and 6.3.1) therefore reduce to the following forms :

$$\left(k\frac{\partial}{\partial t}+k^*\right)\nabla^2 T=\left(1+\tau_q\frac{\partial}{\partial t}\right)\left(\rho c_v\frac{\partial^2 T}{\partial t^2}+\gamma T_0\frac{\partial^2}{\partial t^2}\left(\frac{\partial u}{\partial r}+\frac{u}{r}\right)-\rho\dot{Q}\right) \tag{6.3.5}$$

$$\rho\frac{\partial^2 u}{\partial t^2}=(2\mu+\lambda)(\frac{\partial^2 u}{\partial r^2}+\frac{1}{r}\frac{\partial u}{\partial r}-\frac{u}{r^2})-\gamma\frac{\partial T}{\partial r} \tag{6.3.6}$$

where $\nabla^2=\frac{\partial^2}{\partial r^2}+\frac{1}{r}\frac{\partial}{\partial r}$.

Now, we convert Eqs. (6.3.3-6.3.6) in the non-dimensional forms by using the following notations:

$$(r^*,u^*)=c_0 n(r,u), T^*=\frac{T}{T_0}, (t^*,\tau_0^*,\tau_1^*)=c_0^2\eta(t,\tau_0,\tau_1),$$

$$\left(\sigma_{rr}^{*}, \sigma_{\phi\phi}^{*}\right) = \frac{(\sigma_{rr}, \sigma_{\phi\phi})}{(2\mu+\lambda)}, Q^{*} = \frac{\gamma Q}{k c_0^4 \eta^2}$$

where

$$c_0^2 = \frac{(2\mu+\lambda)}{\rho}, \eta = \frac{\rho c_E}{k}.$$

Therefore, Eqs. (6.3.3-6.3.6) can be reduced to the the following non-dimensional forms (dropping the '$*$' for convenience):

$$\sigma_{rr} = \lambda_1 \frac{\partial u}{\partial r} + \frac{u}{r} - a_1 T \tag{6.3.7}$$

$$\sigma_{\phi\phi} = \frac{\partial u}{\partial r} + \lambda_1 \frac{u}{r} - a_1 T \tag{6.3.8}$$

$$\left(\frac{\partial}{\partial t} + a_0\right) \nabla^2 T = \left(1 + \tau_q \frac{\partial}{\partial t}\right) \left(\frac{\partial^2 T}{\partial t^2} + a_2 \frac{\partial^2}{\partial t^2} \left(\frac{\partial u}{\partial r} + \frac{u}{r}\right) - \frac{1}{a_1} \dot{Q}\right) \tag{6.3.9}$$

$$\frac{\partial^2 u}{\partial t^2} = \frac{\partial}{\partial r} \left(\frac{\partial}{\partial r} + \frac{1}{r}\right) u - a_1 \frac{\partial T}{\partial r} \tag{6.3.10}$$

where

$$a_0 = \frac{k^*}{k c_0^2 \eta}, a_1 = \frac{\gamma T_0}{(2\mu+\lambda)}, a_2 = \frac{\gamma}{\rho c_E}, \lambda_1 = \frac{\lambda}{(2\mu+\lambda)}.$$

Introducing the thermoelastic potential function ψ defined by

$$u = \frac{\partial \psi}{\partial r}, \tag{6.3.11}$$

Eqs. (6.3.9-6.3.10) reduce to

$$\left(\frac{\partial}{\partial t} + a_0\right) \nabla^2 T = \left(1 + \tau_q \frac{\partial}{\partial t}\right) \frac{\partial}{\partial t} \left(\frac{\partial T}{\partial t} + a_2 \frac{\partial}{\partial t} \nabla^2 \psi - \frac{1}{a_1} \dot{Q}\right) \tag{6.3.12}$$

$$\frac{\partial^2 \psi}{\partial t^2} = \nabla^2 \psi - a_1 T \tag{6.3.13}$$

Using Eqs. (6.3.11) and (6.3.13) in Eqs. (6.3.7) and (6.3.8), the components of stress

tensor can be written in terms of ψ as follows:

$$\sigma_{rr} = \left[\left(\frac{\lambda_1 - 1}{r}\right)\frac{\partial}{\partial r} + \frac{\partial^2}{\partial t^2}\right]\psi \tag{6.3.14}$$

$$\sigma_{\phi\phi} = \left[\left(\lambda_1 - 1\right)\frac{\partial^2}{\partial r^2} + \frac{\partial^2}{\partial t^2}\right]\psi \tag{6.3.15}$$

6.4 Conditions

We consider that the body is held at undeformed and unstressed state at the uniform reference temperature T_0 and therefore the initial conditions for all the field variables are taken to be homogeneous. The heat source Q source of strength Q_0, is taken in the form

$$Q = \frac{Q_0}{2\pi r}\delta\left(r\right)H(t) \tag{6.4.1}$$

where $H\left(t\right)$ and $\delta\left(t\right)$ represent Heaviside unit step function and Dirac delta function, respectively.

6.5 Solution in Laplace Transform Domain

In order to solve the problem, we apply the Laplace transform to Eqs. (6.3.12-6.3.15) and using the homogeneous initial conditions and using Eq. (6.4.1), we obtain

$$a_1\bar{T} = \left(\nabla^2 - s^2\right)\bar{\psi} \tag{6.5.1}$$

$$\left(s + a_0\right)\nabla^2\bar{T} = \left(1 + \tau_q s\right)\left(s^2\bar{T} + a_2 s^2\nabla^2\bar{\psi} - A_1\frac{\delta\left(r\right)}{r}\right) \tag{6.5.2}$$

$$\bar{\sigma}_{rr} = \left[\left(\frac{\lambda_1 - 1}{r}\right)\frac{\partial}{\partial r} + s^2\right]\bar{\psi} \tag{6.5.3}$$

$$\bar{\sigma}_{\phi\phi} = \left[(\lambda_1 - 1) \frac{\partial^2}{\partial r^2} + s^2 \right] \bar{\psi} \tag{6.5.4}$$

where $A_1 = \frac{Q_0}{2\pi a_1}$

Replacing $\bar{T}$ from Eq. (6.5.2) by using Eq. (6.5.1), we have

$$\left[\nabla^4 - \left(\frac{b_1 s^3 + b_2 s^2}{s + a_0} \right) \nabla^2 + \left(\frac{1 + \tau_q s}{s + a_0} \right) s^4 \right] \bar{\psi} = - \frac{A_1 a_1 (1 + \tau_q s)}{s + a_0} \frac{\delta (r)}{r} \tag{6.5.5}$$

where $b_1 = 1 + \tau_q (1 + a_1 a_2), b_2 = 1 + a_1 a_2 + a_0$.

We may rewrite the above Eq. in the following form:

$$\left(\nabla^2 - m_1^2 \right) \left(\nabla^2 - m_2^2 \right) \bar{\psi} = - A_2 \frac{\delta (r)}{r} \tag{6.5.6}$$

Here $A_2 = \frac{A_1 a_1 (1 + \tau_q s)}{s + a_0}$, and $m_i^2 \, (i = 1, 2)$ are the roots of the following biquadratic equation:

$$x^2 - \left(\frac{b_1 s^3 + b_2 s^2}{s + a_0} \right) x + \left(\frac{1 + \tau_q s}{s + a_0} \right) s^4 = 0 \tag{6.5.7}$$

The solution of Eqs. (6.5.5) which is bounded at infinity can be obtained as

$$\bar{\psi} (r, s) = \frac{A_2}{m_1^2 - m_2^2} \sum_{i=1}^{2} (-1)^{i-1} k_0 (m_i r) \tag{6.5.8}$$

where $k_0 (m_i r)$ is the modified Bessel function of the second kind.

Now, we calculate the distributions of temperature and displacement by using the relation given by Eq. (6.5.8) in Eq. (6.3.11) and (6.5.1) respectively, and using the following identities:

$$\frac{\partial}{\partial r} k_0 (ar) = - a k_1 (ar), \frac{\partial^2}{\partial r^2} k_0 (ar) = a^2 k_0 (ar) + \frac{a}{r} k_1 (ar), \nabla^2 k_0 (ar) = a^2 k_0 (ar)$$

Therefore, we get

$$\bar{u}(r,s) = \frac{-A_2}{m_1^2 - m_2^2} \sum_{i=1}^{2} (-1)^{i-1} m_i k_0 (m_i r) \tag{6.5.9}$$

$$\bar{T}(r,s) = \frac{-A_2}{a_1 (m_1^2 - m_2^2)} \sum_{i=1}^{2} (-1)^{i-1} \left(m_i^2 - s^2\right) k_0 (m_i r) \tag{6.5.10}$$

Using Eq. (6.5.8) into Eqs. (6.5.3) and (6.5.4), we have the components of stress tensor as

$$\bar{\sigma}_{rr} = \frac{A_2}{m_1^2 - m_2^2} \sum_{i=1}^{2} (-1)^{i-1} \left\{ \left(\frac{\lambda_1 - 1}{r} \right) (-m_i) k_1 (m_i r) + s^2 k_0 (m_i r) \right\} \tag{6.5.11}$$

$$\bar{\sigma}_{\phi\phi} = \frac{A_2}{m_1^2 - m_2^2} \sum_{i=1}^{2} (-1)^{i-1} \left\{ \left(\frac{\lambda_1 - 1}{r} \right) (m_i) k_1 (m_i r) + \left\{ (\lambda_1 - 1) m_i^2 + s^2 \right\} k_0 (m_i r) \right\} \tag{6.5.12}$$

Above solutions determine the expressions for temperature, displacement and stress components in Laplace transform domain (r, s). Due to mathematical complexity in the explicit expressions of fundamental solutions in Laplace transform domain, the determination of analytical solutions in physical domain seems to be a formidabe task. However, in the next section, we facilitate the detailed examination of this model and compare it with other models which are well established in the literature.

6.6 Short-Time Approximated Solution

Practically, this model is applicable only for short duration of time due to the dependency on phase-lag parameters which are of very small values for most of the solid materials. Therefore, the aim of this section is to find the analytical solutions of physical field variables of the present problem for small time by approximating the function as obtained in previous section through Maclaurin's series expansions for large Laplace transform paramter. As described in Chapter 2, after detailed manipulations we find

m_1 and m_2 as the approximated roots of Eq. (6.5.7) for MGT model in the following forms:

$$m_1 = a_{41}s + a_{42} + \frac{a_{43}}{s} \tag{6.6.1}$$

$$m_2 = b_{41}s + b_{42} + \frac{b_{43}}{s} \tag{6.6.2}$$

where

$$a_{41} = \frac{a_{21}a_{31}}{\sqrt{2}}, a_{42} = \frac{a_{21}a_{32} + a_{22}a_{31}}{\sqrt{2}}, a_{43} = \frac{a_{21}a_{33} + a_{22}a_{32} + a_{23}a_{31}}{\sqrt{2}},$$

$$b_{41} = \frac{a_{21}b_{31}}{\sqrt{2}}, b_{42} = \frac{a_{21}b_{32} + a_{22}b_{31}}{\sqrt{2}}, b_{43} = \frac{a_{21}b_{33} + a_{22}b_{32} + a_{23}b_{31}}{\sqrt{2}},$$

$$a_{31} = \sqrt{a_{11}}, a_{32} = \frac{a_{12}}{2\sqrt{a_{11}}}, a_{33} = \frac{-a_{12}a_{12} + 4a_{11}a_{13}}{8\left(a_{11}\right)^{\frac{3}{2}}},$$

$$b_{31} = \sqrt{b_{11}}, b_{32} = \frac{b_{12}}{2\sqrt{b_{11}}}, b_{33} = \frac{-b_{12}b_{12} + 4b_{11}b_{13}}{8\left(b_{11}\right)^{\frac{3}{2}}},$$

$$a_{21} = 1, a_{22} = -\frac{a_0}{2}, a_{23} = \frac{3a_0^2}{8},$$

$$a_{11} = b_1 + \sqrt{b_1^2 - 4\tau_q}, a_{12} = b_2 + \frac{2b_1b_2 - 4\left(\tau_q a_0 + 1\right)}{2\sqrt{b_1^2 - 4\tau_q}},$$

$$a_{13} = \frac{-\left\{2b_1b_2 - 4\left(\tau_q a_0 + 1\right)\right\}^2 + 4\left(b_1^2 - 4\tau_q\right)\left(b_2^2 - 4a_0\right)}{8\left(b_1^2 - 4\tau_q\right)^{\frac{3}{2}}}$$

$$b_{11} = b_1 - \sqrt{b_1^2 - 4\tau_q}, b_{12} = b_2 - \frac{2b_1b_2 - 4\left(\tau_q a_0 + 1\right)}{2\sqrt{b_1^2 - 4\tau_q}},$$

$$b_{13} = -\frac{-\left\{2b_1b_2 - 4\left(\tau_q a_0 + 1\right)\right\}^2 + 4\left(b_1^2 - 4\tau_q\right)\left(b_2^2 - 4a_0\right)}{8\left(b_1^2 - 4\tau_q\right)^{\frac{3}{2}}}$$

Now, substituting the expressions for m_i (i =1,2) from Eqs. (6.6.1) and (6.6.2) into Eqs. (6.5.9-6.5.12) we carry out long and detailed manipulations to obtain the expressions

for fields variables in the Laplace transform domain as

$$\bar{u}\left(r,s\right)=\sqrt{\frac{\pi}{2r}}\left[e^{-m_1 r}\left\{\frac{f_{41}}{s^{\frac{3}{2}}}+\frac{f_{42}}{s^{\frac{5}{2}}}\right\}+e^{-m_2 r}\left\{\frac{f_{43}}{s^{\frac{3}{2}}}+\frac{f_{44}}{s^{\frac{5}{2}}}\right\}\right] \tag{6.6.3}$$

$$\bar{T}\left(r,s\right)=A_1\sqrt{\frac{\pi}{2r}}\left[e^{-m_1 r}\left\{\frac{d_{81}}{s^{\frac{1}{2}}}+\frac{d_{82}}{s^{\frac{3}{2}}}\right\}+e^{-m_2 r}\left\{\frac{d_{83}}{s^{\frac{1}{2}}}+\frac{d_{84}}{s^{\frac{3}{2}}}\right\}\right] \tag{6.6.4}$$

$$\bar{\sigma}_{rr}=A_1\sqrt{\frac{\pi}{2r}}\left[e^{-m_1 r}\left\{\frac{f_{51}}{s^{\frac{1}{2}}}+\frac{f_{52}}{s^{\frac{3}{2}}}\right\}+e^{-m_2 r}\left\{\frac{f_{61}}{s^{\frac{1}{2}}}+\frac{f_{62}}{s^{\frac{3}{2}}}\right\}\right] \tag{6.6.5}$$

$$\bar{\sigma}_{\phi\phi}=A_1\sqrt{\frac{\pi}{2r}}\left[e^{-m_1 r}\left\{\frac{h_{31}}{s^{\frac{1}{2}}}+\frac{h_{32}}{s^{\frac{3}{2}}}\right\}+e^{-m_2 r}\left\{\frac{h_{41}}{s^{\frac{1}{2}}}+\frac{h_{42}}{s^{\frac{3}{2}}}\right\}\right] \tag{6.6.6}$$

Here, the different notations used in above expressions are provided in Appendix III. Next, taking the inverse Laplace transforms of Eqs. (6.6.3-6.6.6) and using the following identities

$$L^{-1}\left(\frac{e^{\frac{-a}{s}}}{s^{\frac{3}{2}}}\right)=\frac{sin\left(2\sqrt{at}\right)}{\sqrt{a\pi}},a>0,$$

$$L^{-1}\left(\frac{e^{\frac{-a}{s}}}{s^{\frac{5}{2}}}\right)=\frac{sin\left(2\sqrt{at}\right)}{2\sqrt{\pi}a^{\frac{3}{2}}}-\frac{t^{\frac{1}{2}}cos\left(2\sqrt{at}\right)}{\sqrt{\pi}a},a>0,$$

$$L^{-1}\left(\frac{e^{\frac{-a}{s}}}{s^{\frac{1}{2}}}\right)=\frac{cos\left(2\sqrt{at}\right)}{\sqrt{\pi t}},a>0,$$

we get

$$\begin{aligned}u(r,t)=A_1\sqrt{\frac{\pi}{2r}}\Bigg[e^{-a_{42}r}\Bigg\{f_{41}\frac{sin\left(2\sqrt{k_{12}(t-k_{11})}\right)}{\sqrt{k_{12}\pi}}+f_{42}\Bigg(\frac{sin\left(2\sqrt{k_{12}(t-k_{11})}\right)}{2k_{12}^{\frac{3}{2}}\sqrt{\pi}}-\\ \frac{(t-k_{11})^{\frac{1}{2}}cos\left(2\sqrt{k_{12}(t-k_{11})}\right)}{k_{12}\sqrt{\pi}}\Bigg)\Bigg\}H(t-k_{11})+e^{-b_{42}r}\Bigg\{f_{43}\frac{sin\left(2\sqrt{k_{22}(t-k_{21})}\right)}{\sqrt{k_{22}\pi}}\\ +f_{44}\Bigg(\frac{sin\left(2\sqrt{k_{22}(t-k_{21})}\right)}{2k_{22}^{\frac{3}{2}}\sqrt{\pi}}-\frac{(t-k_{21})^{\frac{1}{2}}cos\left(2\sqrt{k_{22}(t-k_{21})}\right)}{k_{22}\sqrt{\pi}}\Bigg)\Bigg\}H(t-k_{21})\Bigg]\end{aligned} \tag{6.6.7}$$

$$T(r,t) = A_1\sqrt{\frac{\pi}{2r}}\left[e^{-a_{42}r}\left\{d_{81}\frac{cos\left(2\sqrt{k_{12}(t-k_{11})}\right)}{\sqrt{\pi(t-k_{11})}} + d_{82}\frac{sin\left(2\sqrt{k_{12}(t-k_{11})}\right)}{\sqrt{k_{12}\pi}}\right\}H(t-k_{11})\right.$$
$$\left.+e^{-b_{42}r}\left\{d_{83}\frac{cos\left(2\sqrt{k_{22}(t-k_{21})}\right)}{\sqrt{\pi(t-k_{21})}} + d_{84}\frac{sin\left(2\sqrt{k_{22}(t-k_{21})}\right)}{\sqrt{k_{22}\pi}}\right\}H(t-k_{21})\right] \quad (6.6.8)$$

$$\sigma_{rr}(r,t) = A_1\sqrt{\frac{\pi}{2r}}\left[e^{-a_{42}r}\left\{g_{51}\frac{cos\left(2\sqrt{k_{12}(t-k_{11})}\right)}{\sqrt{\pi(t-k_{11})}} + g_{52}\frac{sin\left(2\sqrt{k_{12}(t-k_{11})}\right)}{\sqrt{k_{12}\pi}}\right\}H(t-k_{11})\right.$$
$$\left.+e^{-b_{42}r}*\left\{g_{71}\frac{cos\left(2\sqrt{k_{22}(t-k_{21})}\right)}{\sqrt{\pi(t-k_{21})}} + g_{72}\frac{sin\left(2\sqrt{k_{22}(t-k_{21})}\right)}{\sqrt{k_{22}\pi}}\right\}H(t-k_{21})\right] \quad (6.6.9)$$

$$\sigma_{\phi\phi}(r,t) = A_1\sqrt{\frac{\pi}{2r}}\left[e^{-a_{42}r}\left\{h_{31}\frac{cos\left(2\sqrt{k_{12}(t-k_{11})}\right)}{\sqrt{\pi(t-k_{11})}} + h_{32}\frac{sin\left(2\sqrt{k_{12}(t-k_{11})}\right)}{\sqrt{k_{12}\pi}}\right\}H(t-k_{11})\right.$$
$$\left.+e^{-b_{42}r}*\left\{h_{41}\frac{cos\left(2\sqrt{k_{22}(t-k_{21})}\right)}{\sqrt{\pi(t-k_{21})}} + h_{42}\frac{sin\left(2\sqrt{k_{22}(t-k_{21})}\right)}{\sqrt{k_{22}\pi}}\right\}H(t-k_{21})\right] \quad (6.6.10)$$

where $k_{11} = a_{41}r$, $k_{12} = a_{43}r$, $k_{21} = b_{41}r$, $k_{22} = b_{43}r$.

Eqs. (6.6.7-6.6.10) represent the final solution of the present problem and give the expressions for the distributions of field variables in physical domain.

6.7 Analysis of Analytical Results

The short-time approximated solutions for the field variables given by Eqs. (6.6.7-6.6.10), it is observed that the solution of each field variable consists of two coupled waves and that are expressed by adjoining two expressions. The first expression, containing the term $H(t - a_{41}r)$ represents the wave that is propagating with finite velocity $1/a_{41}$ near the wavefront $r = t/a_{41}$ and the wave decays exponentially with an attenuation coefficient a_{42}. Another expression, containing the term $H(t - b_{41}r)$ identifies another wave propagating with finite velocity $1/b_{41}$ near the wavefront $r = t/b_{41}$ and this wave also decays exponentially with an attenuation coefficient b_{42}. It is clearly

noted that the decay coefficient and velocity of both the waves depend on material parameters as well as on the relaxation time parameter. Furthermore, it is investigated from the analytical solutions that the displacement distribution is continuous, but temperature and stress components suffer infinite discontinuity at both the wavefronts at $t = k_{11}$ and $t = k_{21}$. Here k_{11} and k_{21} are linear functions of radial distance r, and therefore the point of discontinuity changes with time. Consequently, it can be concluded from the solutions given by Eqs. (6.6.7-6.6.10) that at any given instant of time t, the disturbance inside the medium can be observed only upto the particular distance $max\{t/k_{11}, t/k_{21}\}$ and beyond this region no disturbance can be observed. Thus this result affirms that the effect of the heat source are confined upto a finite region of space surrounding the source. Hence, unlike the MGL theory, the new model of thermoelasticity (QMGT model) that is considered in the present Chapter clearly admits the finite speed of disturbance and finite domain of influence. This observation perfectly matches with the domain of influence results for this theory as reported by Jangid and Mukhopadhyay (2021).

By comparing our results with the corresponding results predicted by other theories, it must be pointed out that in the case of GN-III model, Dhaliwal et al. (1997) had reported that the solution for each field consists of two parts, the first part indicating the wave nature that decay exponentially with radial distance and another part is diffusive in nature which shows infinite speed of heat propagation. Hence, we conclude that the QMGT model eliminates the unrealistic prediction of infinite speed of heat propagation as observed in the context of GN III model. In the GN III model, authors have further indicated that temperature, stress components are continuous in nature.

In the case of LS model as investigated by Sherief and Anwar (1986) and in case of GL model as studied by Ezzat (1995) and also by Chandrasekharaiah and Murthy (1991), one can find that the solution for each field consists of superposition of two waves, both propagating with finite velocity and decaying exponentially with radial

distance. Furthermore, in case of LS model, Sherief and Anwar (1986) have indicated that temperature and stress components are discontinuous in nature showing infinite jump discontinuities at the two wave fronts. However, in case of the GL model as reported (Ezzat (1995); Chandrasekharaiah and Murthy (1991)), the temperature field shows finite jump discontinuity, but radial and circumferential stress components have infinite jump discontinuities at the wavefronts. Interestingly, in the context of GN-II model it has been reported by Chandrasekharaiah and Srinath (1998) that the solution of each field consists of two undamped waves both propagating with finite speed but without any decay coefficient. Infinite jump discontinuities at the wave fronts by temperature and stress fields are also observed in this case. Hence, it can be concluded that the new model admits finite speed of elastic and thermal waves like LS and GL and GN-II theories, but predicts more similar behaviour of field variables like LS model.

6.8 Numerical Results & Discussion

In this section, an attempt is made at illustrating the analytical results obtained in the previous section and compare the results under present study with the corresponding results in the contexts of other models (Sherief and Anwar (1986); Dhaliwal et al. (1997); Chandrasekharaiah and Srinath (1998); Ezzat (1995); Prasad et al. (2011)), which are well established in the literature. The material property of copper is chosen for the thermoelastic analysis. The physical data for such material is given in Chapter 2. We assume the values of phase-lag parameters as $\tau_q = 0.2$ (dimensionless) and $k^* = 500\mathrm{Wm}^{-1}\mathrm{K}^{-1}$.

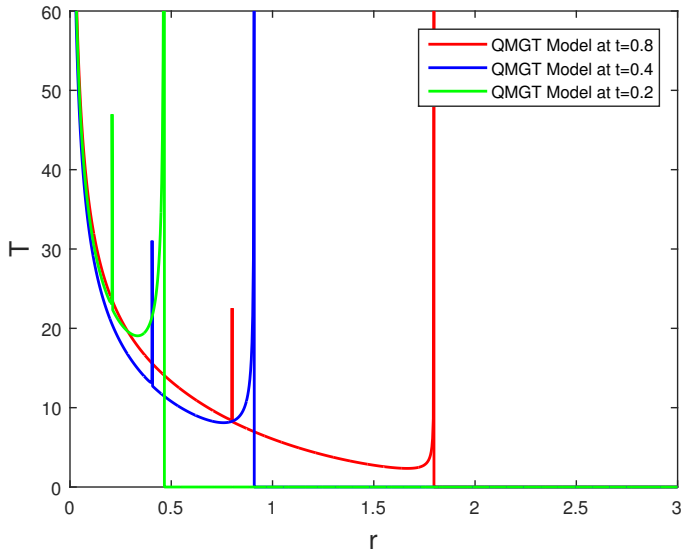

Figure 6.8.1: Variation of temperature (T) at three different times

Figure (6.8.1-6.8.4) represent the variations of the dimensionless field quantities such as temperature, displacement, and stress components with respect to radial distance at three different instants of time ($t = 0.2, 0.4, 0.8$). We find that the elastic and thermal wavefront is located at points $r = 0.2$ and $r = 0.45$ respectively at time $t = 0.16$. Similarly we observe $(0.4, 0.9)$,and $(0.8, 1.79)$ are the points for elastic and thermal wavefront at non-dimensional time 0.4 and 0.8 respectively. We find that the non-dimensional speed of the slower wave (elastic) and the faster wave (thermal) are 0.99 and 2.24, respectively. The radial distributions of different field variables are plotted in different figures which demonstrate that each of the four fields shows an infinite jump at the origin which is the position of heat source and this effect decreases with time. Further, it can be observed that the field variables show no effect beyond the thermal wavefront. This is completely in agreement with our theoretical results given in Eqs. (6.6.7-6.6.10). We further notice the following important observations:

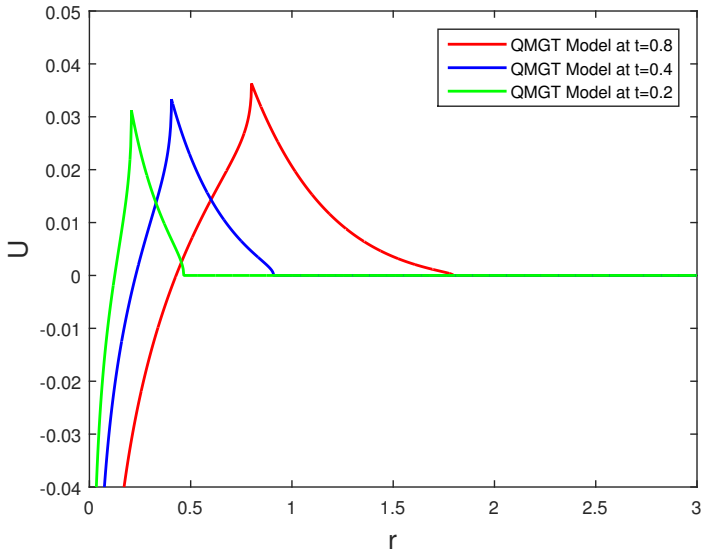

Figure 6.8.2: Variation of displacement (U) at three different times

In figure (6.8.1), that represents the temperature distribution with radial distance (r) at three different instant of times, indicate that the temperature field decreases from very high value to zero as r increases. However, just behind the position of elastic and thermal wavefronts, the temperature suddenly starts increasing and reaches to a very high value at both the wavefront positions and also no disturbance is observed beyond the thermal wavefront. Thus, the heat source's effects are confined to a bounded but time-dependent region of space surrounding the heat source. In the GN II model, as reported by Chandrasekharaiah and Srinath (1998), the temperature field increases in the region between source and the position of elastic wavefront. Here, GN II model gives finite value of temperature at $r = 0$, which is quite unusual behaviour for a continuous line heat source. However, in the context of GN III model (Dhaliwal et al. (1997)), authors had shown that temperature field decreases from infinity (at $r = 0$) to zero as r tends to infinity. This model shows different behaviour corresponding to QMGT model, as GN III model gives infinite domain of influence. On the other hand, in the cases of LS model (Sherief and Anwar (1986)) and GL model (Ezzat (1995)), the same

behaviour for temperature field has been observed with a significant difference that in case of GL model, the field shows finite jump discontinuity at the wavefronts, whereas LS model predicts infinite jump discontinuity at the wavefronts and this fact completely matches with the results of the present case. However, after the location of thermal wavefront, no disturbance has been observed for LS as well as for GL models, like the QMGT model.

Figure (6.8.2) shows that displacement curve is continuous and its effect has been confined to time-dependent finite region. It is also noted that displacement increases from very high negative value at origin ($r = 0$) to a maximum value near the location of thermal wavefront and then starts decreasing and finally reaches to zero value. A similar behaviour of this field has been found in the case of other models as mentioned above.

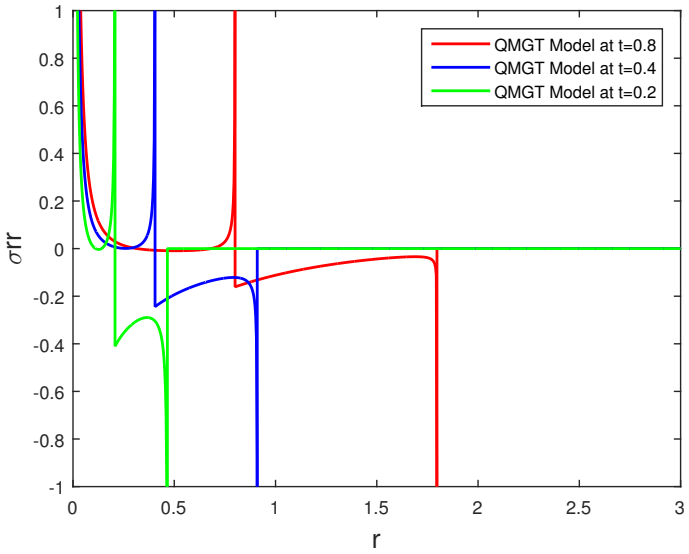

Figure 6.8.3: Variation of radial stress (σ_{rr}) at three different times

Figure (6.8.3) shows the variation of the radial stress with radial distance at three different instants of time $(0.2, 0.4, 0.8)$. One can note that between the location of

heat source and elastic wavefront, the radial stress is tensile. Whereas the compressive stress is occurring in other parts. However, just before the position of elastic and thermal wavefront, the radial stress suddenly starts increasing and reaches to very high numerical value. Further, we note that no disturbance can be observed beyond the thermal wavefront. This field also indicates discontinuity at both the wavefronts and also shows quite similar behaviour in the close neighbourhood of the wavefronts under GN II model (Chandrasekharaiah and Srinath (1998)). In this case also the compressive stress is observed in the region between the two wavefronts. In the case of LS model (1986), both compressive and tensile stresses are observed in the region between heat source and elastic wavefront. Whereas similar behaviour to QMGT model are observed in the region between two the wavefronts. In case of the GL model (Ezzat (1995)), the nature of stress field is similar to QMGT model. However finite jump discontinuities are observed at both the wavefronts under GL model. Beyond the thermal wavefront, no effect has been observed for LS and GL models as reported in literature.

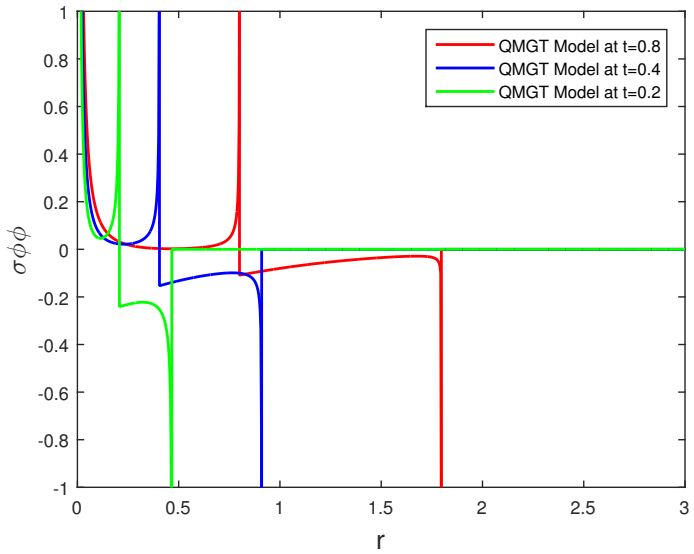

Figure 6.8.4: Variation of circumferential stress ($\sigma_{\varphi\varphi}$) at three different times

Figure (6.8.4) reveals that the circumferential stress is tensile in the region between heat source and elastic wavefront, but compressive in the region between the wavefronts. Also, circumferential stress decreases in the region between the source and elastic wavefront, but it starts increasing in a region just behind the wavefront and reaches to a very high magnitude. Beyond the elastic wavefront, the circumferential stress starts with finite value and decreases but at the points very close to T-wavefront (thermal), it again achieves very high value of compression. Beyond this point, no effect of this field is observed. This field also indicates discontinuity at both the wavefronts and also shows quite similar behaviour in the neighbourhood of wavefronts like the case of GN II model as shown by Chandrasekharaiah and Srinath (1998). Compressive nature of stress can be observed in between the wavefront regions. In LS model (Sherief and Anwar (1986)), the behaviour of stress field shows different behaviour as compared to QMGT model, since compressive stress is observed in the region upto the elastic wave front. It also shows quite opposite nature at $r = 0$. Further, the compressive stress has been observed in the region between the two wavefronts. In case of GL model (Ezzat (1995)) a similar prediction like LS and QMGT model is indicated showing an infinite jump discontinuity at both the wave fronts and no effect of disturbance can be observed beyond the thermal wavefront. It must be pointed out here that GN-II model (Chandrasekharaiah and Srinath (1998)) is in agreement with LS, GL and QMGT model in this respect as compared to GN-III model which predicted continuous nature of all field variables.

6.9 Conclusion

In this Chapter of the thesis, the investigation focuses on the analysis of thermoelastic effects using the Moore-Gibson-Thompson thermoelasticity theory due to the presence of a continuous line heat source in an infinite medium. This study enlighten some

similarities and dissimilarities between the predictions of the recently proposed QMGT theory with well established corresponding results under other existing theories (LS, GL, GN). The characteristic features of the present investigation may be summarized as follows:

- The analytical solutions obtained for short time in the context of QMGT model reveals that the solution for each field consists of superposition of two waves, both propagating with finite velocity and with an exponential decay. The relaxation time parameter as well as material property have prominent effect on velocity and decay coefficients of the waves.

- Like LS, GL and GN-II theories, the QMGT model predicts that the effect of the continuous line heat source is confined to a time-dependent bounded region of the space surrounding the heat source. However, the elastic and thermal waves in the present case are damped in nature. This is further in agreement with the results under LS and GL models, but it is unlike the case of GN-II model which shows undamped wave propagation.

- For the cases of LS, GL, GN-II and QMGT models, the temperature and stress components are discontinuous, unlikely for GN-III model which predicts the physical field variables to be continuous. However, like the case of LS theory and GN-II theory, we obtain infinite jump discontinuity of temperature and stress distributions at the elastic and thermal wavefronts under the new theory (QMGT), as compared to the case of GL model where the temperature is discontinuous with finite jump and stress fields show infinite jump discontinuities at the wave fronts.

- The new thermoelasticity theory is a realistic model like the LS and GL theories, although the new model shows much similar features like the LS model.

- The predictions of responses due to continuous line heat source by the two new theories (the QMGT theory and MGL theory) considered in the present thesis

are significantly different. QMGT theory shows more realistic results as compared to the MGL theory which indicates an infinite speed of thermomechanical disturbances like the classical theory of thermoelasticity and viscoelasticity.